Simple procedure for vacant POMs-stabilized palladium (0) nanoparticles in water: structural and dispersive effects of lacunary polyoxometalates

R. Villanneau, A. Roucoux, P. Beaunier, D. Brouri, A. Proust

Journal Name

ARTICLE

Simple procedure for vacant POMs-stabilized palladium (0) nanoparticles in water: structural and dispersive effects of lacunary polyoxometalates

R. Villanneau,*[a,b] A. Roucoux,*[c,d] P. Beaunier,[e,f] D. Brouri[e,f] and A. Proust[a,b]

Metallic palladium nanoparticles have been generated by hydrogenation with H_2 of solutions of several non organometallic Pd^{II}-derivatives of heteropolytungstates, at ambient temperature and atmospheric pressure. These nanoparticles have been characterized by various techniques: ^{31}P NMR and Raman spectroscopy, TEM (including cryogenic techniques), DLS, EDX and XPS. The present strategy ruled out the presence of other ligands and/or stabilizing agents other than the lacunary polyoxometalates (POMs) used. This allows the evaluation of the true efficiency of the different vacant POMs for the stabilization of the nanoparticles.

1. Introduction

The pioneering catalytic reduction of nitrobenzene described by Nord[1] may be seen as the starting point of the extensive use of metallic nanoparticles (NPs) as reduction (mostly hydrogenation) catalysts.[2] However, recent examples, especially in the chemistry of noble-metals-based (Au, Pd, Ru, Pt) NPs, have shown attractive perspectives in the field of mild oxidation catalysis.[3] Among all molecular oxidants available, dioxygen can reasonably be considered as the cleanest and cheapest one. Indeed, O_2 (or *a fortiori* air) is the most attractive reagent owing to its high content of active oxygen and to the co-production of only water in most catalytic processes (no by-products in some cases), especially in aqueous media. However it is hard to activate so that a lot of oxidation reactions are kinetically inhibited under relatively mild conditions.

One of the valuable methods to form activated dioxygen is the combination of O_2 and noble metal Nps. Thanks to high surface area-to-volume ratios providing an increased number of potential active sites, metal NPs are also generally considered as ideal materials for application in catalysis. Amongst noble metal nanoparticles, Ru(0) or Pd(0) NPs have been investigated with success for the aerobic catalytic selective conversion of primary alcohols (especially benzylic alcohols) to aldehydes. In this field, the selectivity towards aldehyde has been particularly underlined since usual oxidation of primary alcohols in water mainly yields carboxylic derivatives.[4]

In the context of such studies, the use of stabilizing agents for NPs adapted to oxidation reactions in water appears as an obvious goal. Among all stabilizing agents tested (such as polymers, cyclodextrins, surfactants or water-soluble ligands), polyoxometalates (POMs) are pointed out, due to several convergent properties that make them considered as choice candidates. POMs are indeed transition metal oxo-clusters, where the metal ions (in particular, W or Mo) are at their highest oxidation states.[5] Depending on the counter-ions associated, they can be used either in water (with alkaline ions) or in organic medium (with tetraalkylammonium for instance). They are generally stable against oxidation, even at high temperature, and hydrolysis, providing that pH conditions are controlled. Owing to these properties, the literature involving their use as oxidation catalysts is abundant,[6,7,8,9] including the use of dioxygen as the oxidant.[10]

In addition, due to the combination of their negative charges (especially in the case of lacunary species) and large relative sizes, they have been used as promising stabilizing agents for metallic NPs in solution,[11,12] having in mind that a sensible choice of the stabilizing POMs would also open the door to applications in bifunctional catalysis. The considerable pioneering works of R.G. Finke at Colorado State University, based on the reduction of organometallic derivatives of POMs, had demonstrated the feasibility of the association of POMs and NPs in organic medium.[13] In a previous work, we also used organometallic derivatives of POMs for the generation of Ru^0 NPs supported on SBA-15.[14] Thereafter, numbers of studies have been performed and several other strategies so far employed that can be summed up as followed:
- the reduction of (often commercially available) metallic salts of noble-metals ions by a chemical reagent (H_2, $NaBH_4$…) in the presence of in general nonvacant POMs,[15]
- the reduction of metallic salts of noble-metals ions by reduced POMs, the latter playing the role of the reducing and stabilizing (once re-oxidized) reagent at once,[11,16]
- the reduction of a metallic salt of the targeted metal by photoreduced POMs, in the presence of an organic sacrificial donor (typically an alcohol). In this case, the POMs are first

photoreduced, the POMs in their excited state playing the role of the oxidants towards the organic donor and the reducing agents for the generation of the NPs at once.[11,17]

- the exchange of the stabilizing agents of preformed metallic NPs (including bimetallic NPs) with POMs.[18]

In most cases (except in Finke's work), the studies have been performed in water. Furthermore, many have been done in the presence of other ligands (such as chloride) or of tetraalkylammonium counter-ions, known for stabilizing metallic NPs, so that the intrinsic role of the POMs is sometimes somewhat questionable.

In the present work, we have focused on the capacity of lacunary POMs to efficiently stabilize zerovalent Pd NPs. Structural and dispersive effects of various vacant POMs have been thus investigated. The one-pot strategy used here is based on the hydrogenation in very mild conditions of aqueous solutions of non-organometallic Pd^{II}-derivatives of POMs (Pd^{II}-POMs). It is noteworthy that this strategy has been used in the case of water-soluble noble-metal derivatives of POMs.[19] In our study, various water-soluble Pd^{II}-derivatives of heteropolytungstates have been surveyed in order to check the effect of the nature of the POMs on the stability of the Pd^0 NPs formed in solution. Among the Pd^{II}-POMs tested, we have focused on the behavior of three particular anions, $[Pd_2\{PW_{11}O_{39}\}_2]^{10-}$, $[Pd\{As_2W_{19}O_{67}(H_2O)\}]^{12-}$ and $[Pd_2\{P_2W_{19}O_{69}(H_2O)\}]^{10-}$ (respectively anions of **3**, **4** and **5** fig. 1). The present work allowed an unambiguous evaluation of the stabilizing efficiency of the different lacunary POMs tested, since the nanoparticles were formed in the absence of other co-stabilizers.
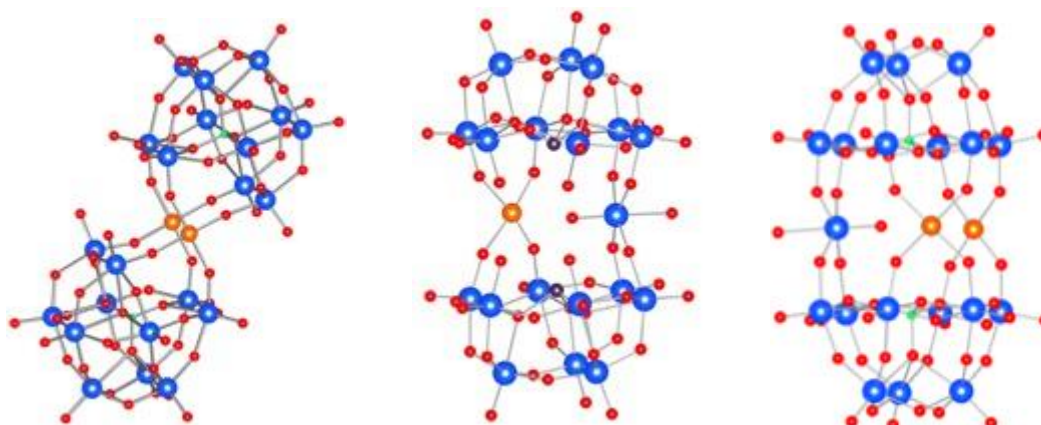

Fig. 1 structural representation of $[Pd_2\{PW_{11}O_{39}\}_2]^{10-}$, anion of **3** (left), $[Pd\{As_2W_{19}O_{67}(H_2O)\}]^{12-}$, anion of **4** (middle) and $[Pd_2\{P_2W_{19}O_{69}(H_2O)\}]^{10-}$, anion of **5** (right). O atoms are in red, W in blue, P in green, As in dark purple and Pd in orange.

2. Experimental

2.1 Materials and methods

All Pd^{II}-POMs precursors $K_8[Pd\{P_2W_{20}O_{70}(H_2O)\}]\cdot20H_2O^{20}$ (**1**) $K_{12}[Pd_3\{PW_9O_{34}\}_2]\cdot30H_2O^{20}$ (**2**) and $K_9H[Pd_2\{PW_{11}O_{39}\}_2]\cdot37H_2O$ [21] (**3**) and $K_{10}[Pd_2\{P_2W_{19}O_{69}(H_2O)\}]\cdot30H_2O^{20}$ (**5**) were prepared according to the literature. All characterizations were in accordance with those described in the respective publications. The preparation of compound $Cs_7K_{1.5}Na_3H_{0.5}[Pd\{As_2W_{19}O_{67}(H_2O)\}]\approx20H_2O^{\dagger}$ (**4**) was adapted from the literature.[22]

All reagents were obtained from commercial sources and used as received. IR spectra were recorded from KBr pellets on a Biorad FT 165 spectrometer. Raman spectra were recorded on solid samples on a Kaiser Optical Systems HL5R spectrometer equipped with a near-IR laser diode working at 785 nm. The ^{31}P NMR (121.5 MHz) solution spectra were recorded in 5 mm o.d. tubes on a Bruker Avance 300 spectrometer equipped with a QNP probehead. Chemical shifts are referenced with respect to external 85% H_3PO_4, and were measured by the substitution method. Flows of H_2 were obtained with an F•DBS PGH$_2$ 500 hydrogen generator.

TEM analyses were realized on a microscope operating at 200 kV with a resolution of 0.18 nm (JEOL JEM 2011 UHR) equipped with an EDX system (PGT IMIX-PC). Sample preparations consists of an ultrasonic dispersion of the samples in water, and a deposition of few drops on a Cu grid covered with amorphous carbon film.

Cryo-TEM analyses were realized on a microscope operating at 200 kV (JEOL 2100). A drop of the solution is deposited on a holey carbon grid and frozen at liquid nitrogen. Elemental analyses were performed by the Service Central d'Analyse of the CNRS (Villeurbanne, France).

X-ray photoelectron spectroscopy (XPS) spectrum were performed on an Omicron (ESCA+) spectrometer, using an Al Kα X-ray source (1486.6 eV) equipped with a flood gun.

2.2 Preparation of the POMs-stabilized nanoparticles suspension

In a typical experiment, a solution of $K_9H[Pd_2\{PW_{11}O_{39}\}_2]\cdot37H_2O$ ($1.27\cdot10^{-5}$ mol, 0.084 g, corresponding to $\approx 2.50\cdot10^{-3}$ mol L^{-1} of Pd^{II}) in 10 mL of

deionized water was prepared and degased using conventional schlenk techniques. This solution was then exposed to a flow of H_2 (1 bar) during 1 h, during which the orange solution turned to a black suspension of stabilized Pd^0 nanoparticles. At this step, no aggregates were visually observed.

For the other compounds, the mass of Pd^{II}-POMs precursors was adapted in order to get a concentration of Pd^{II} in solution equal to $2.50 \cdot 10^{-3}$ mol L^{-1}.

3. Results and discussion

3.1 Preparation of the nanoparticles suspensions.

Hydrogenation in mild conditions (room temperature and exposure to a gentle stream of H_2) of aqueous solutions of all Pd^{II}-POMs tested (compounds **1** to **5**) led systematically to the reduction of the Pd^{II} cations coordinated by the different lacunary POMs. This reduction required the absence of O_2, and the samples have been placed under Ar prior to the introduction of H_2. It is noteworthy that a previous work mentioned the formation of Pd^0 NPs by hydrogenation of a Pd^{II}-POM, described as an hypothetical $K_5[PdPW_{11}O_{39}] \cdot 12H_2O$.[19, 23] However, the very strong conditions used (200 °C under 30 bar H_2) had led to the reduction of both POMs and Pd^{2+} ions and the precipitation of ill-defined highly reduced materials.

In our case, we observed the formation of dark suspensions of Pd^0 nanoparticles within approximately 1h with each Pd^{II}-POM tested. The reduction of the Pd^{2+} ions into metallic Pd^0 afforded protons that induced the acidification of the suspension (final pH = 3.40 with compound **3**). We found that the stability of these suspensions was dependent on the nature of the complexing POMs in solution. Indeed, while the suspensions were stable over several weeks when starting with $[Pd_2\{PW_{11}O_{39}\}_2]^{10-}$ (anion of **3**) and $[Pd\{As_2W_{19}O_{67}(H_2O)\}]^{12-}$ (anion of **4**), we observed the rapid precipitation of the particles with all other Pd^{II}-POMs tested (compounds **1**, **2** and **5**). In the

case of $[Pd_2\{P_2W_{19}O_{69}(H_2O)\}]^{14-}$ (anion of **5**), the precipitation was however not immediate, so that TEM micrographs of the suspension of NPs could have been recorded (see fig 2).

In addition, in the case of the NPs obtained from compound **3** we have checked the completion of the reaction by ^{31}P NMR spectroscopy. After one hour of reaction, we observed the complete disappearance of the signal attributed to $[Pd_2\{PW_{11}O_{39}\}_2]^{10-}$ and the presence of a single peak at -10.85 ppm, assigned to free $[PW_{11}O_{39}]^{7-}$ sub-units. In order to make the link between the size of the NPs in the solid-state and in solution, ^{31}P DOSY NMR experiments were also performed. However, due to the relatively low POMs concentration of the suspensions, we were not able to determine suitable diffusion coefficients for the $[PW_{11}O_{39}]^{7-}$-containing entities in solution.

If we compared all tested compounds, the stability of the obtained suspensions can tentatively be paralleled to the stability of the complexing POMs in water. Indeed, regarding the literature concerning the phosphotungstates derivatives, it is admitted that this stability (in particular in acidic pH) follows the series:
α-$[PW_{11}O_{39}]^{7-}$ > $[P_2W_{19}O_{69}(H_2O)]^{14-}$ > $[P_2W_{20}O_{70}(H_2O)_2]^{10-}$ >> α-$[PW_9O_{34}]^{12-}$.[24] Considering the fairly good metastability of the arsenic-containing $[As_2W_{19}O_{67}(H_2O)]^{14-}$ anion, the formation of stable NPs suspension starting with **4** was expected, even if the observed shapes of the NPs could indicate a weaker stabilization than with **3** (see below).

3.2 Transmission Electronic Microscopy characterization of the nanoparticles

Figure 2 displayed the electron micrographs (TEM) of nanoparticles obtained by reduction with H_2 of $K_9H[Pd_2\{PW_{11}O_{39}\}_2] \cdot 37H_2O$ (**3**), $Cs_7K_{1.5}Na_3H_{0.5}[Pd\{As_2W_{19}O_{67}(H_2O)\}] \approx 20H_2O$ (**4**) and $K_{10}[Pd_2\{P_2W_{19}O_{69}(H_2O)\}] \cdot 30H_2O$ (**5**).
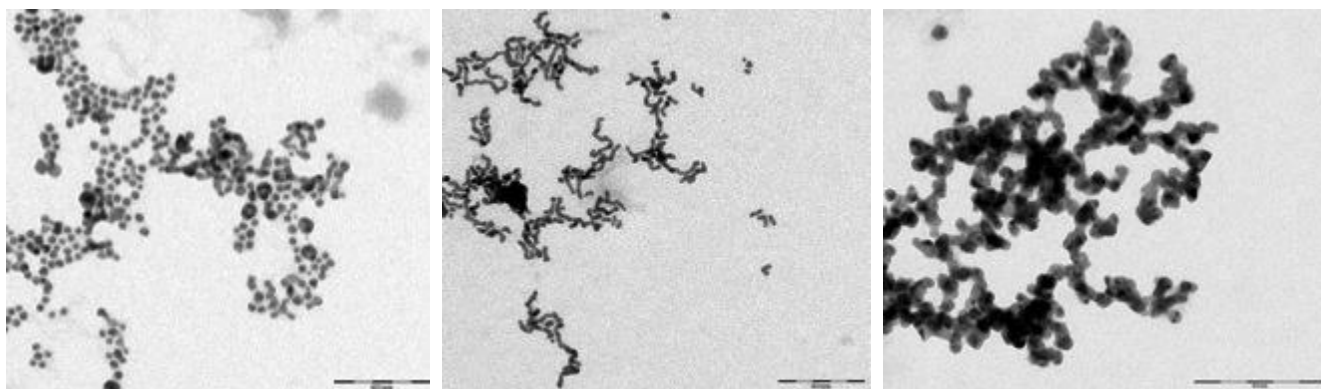

Fig.2 TEM micrographs of Nps obtained by hydrogenation of **3** (left) and **4** (middle) and **5** (right). The scale bar in the right corner corresponds to 100 nm.

Figure 2 (left) showed that most metallic Pd^0 obtained from **3** crystallized in the form of globular particles with an average diameter of 7.9±1.6nm as shown on the size histogram which results from the measurement of about 450 particles. The

particles contain an average number of 80000 atoms. Figure 3 shows the obtained particle size distribution, which can be well fitted by a Gaussian curve. The chemical analysis obtained for the precipitated $[PW_{11}O_{39}]^{7-}$-stabilized NPs (see paragraph 3.4

Raman spectroscopy for the experimental details) indicated that the average Pd/W ratio in this solid sample is equal to 1.61 (%Pd = 29.4 and %W = 31.55). Considering the average number of Pd atoms per NP, we then calculated the following composition of the materials: $Pd(0)_{80000}\sim\{[PW_{11}O_{39}]^{7-}\}_{\approx4500}$. This can be compared to the average composition of Finke's Ir(0) systems:[13] $Ir(0)_{300}\sim\{[P_4W_{30}Nb_6O_{123}]^{16-}\}_{\approx33}$, corresponding to a ratio Ir/(W+Nb) = 0.252 for smaller particles (2.03 ± 0.28 nm). A closer inspection of the sample revealed that some particles have regular shapes (triangle- or diamond-shaped). In the HR-TEM micrographs on fig. 4, lattice fringes were clearly observed, but the presence of different domains in most NPs showed that they are polycrystalline. The inter-reticular distances (respectively 2.240 and 1.945 Å) from FFT are close to those of [111] and [200] Pd^0 FCC planes.

Examination of the elemental composition of the samples by X-ray energy dispersive spectroscopy (XEDS) indicated that all the Pd present in the solid was concentrated exclusively in the NPs (fig. S2). Additionally, this also indicated that the reduction of the Pd^{II} incorporated in the POMs was a rapid (less than 1h) and efficient reaction even in the very mild conditions used. Furthermore XED spectrum on a single NP also revealed the presence of W and K, indicating the presence of POMs at the surface of the NPs. The presence of the POMs was also detected in the amorphous materials around the NPs.

Figure 2 (middle) displayed the electron micrographs of the NPs obtained from compound **4**. Unlike the previous system, these NPs were found to be worm-like, with an average width of approximately 4 nm and lengths up to 40 nm. This very particular NP form indicates generally a weak stabilization of the NP.
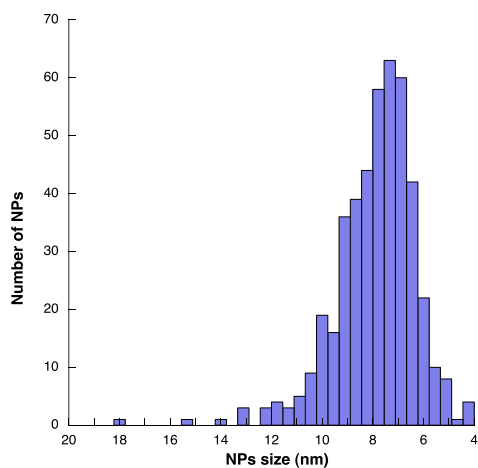

Fig. 3 Size histogram for Pd^0 NPs obtained by hydrogenation of compound **3**.

Finally, the micrograph of freshly prepared suspensions of the NPs obtained from **5** (Fig. 2, right) clearly showed an important coalescence of these Nps, and the formation of a disordered "network". In this case, despite diameters (about 10 nm) similar to those obtained with compound **1**, the Nps started to aggregate immediately after their formation, leading to their coagulation within a few hours.
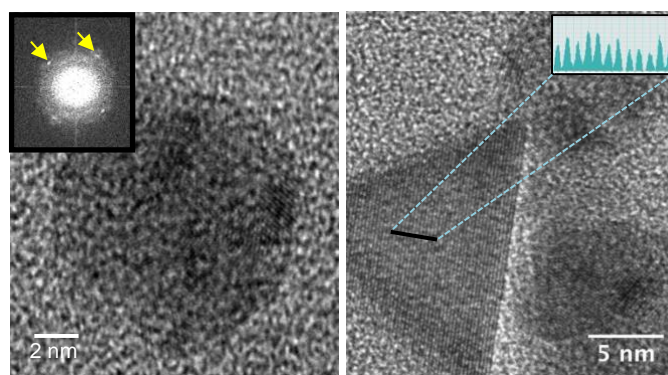

Fig 4: HR-TEM micrograph of a Pd^0 nanoparticle obtained from **3**.

3.3 Dynamic Light Scattering measurements

The DLS analysis (fig 5) was performed on a freshly prepared suspension of $\{PW_{11}O_{39}\}^{7-}$-stabilized Pd^0 NPs. In this case, we observed that the particles have a hydrodynamic diameter centered at 13.5 nm. This is in accordance with the size of the nanoparticles observed by TEM or HR-TEM. Dilution by 4 of this solution did not modify substantially the position of the maximum of the peak. This indicates that the effect of the concentration of NPs seems to have no effect on their size and/or the aggregation process.
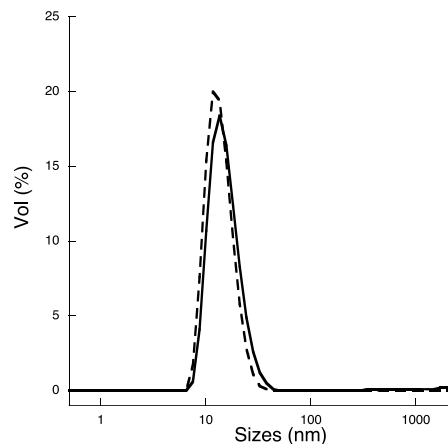

Fig. 5 DLS curve for $\{PW_{11}O_{39}\}^{7-}$-stabilized Pd^0 NPs at $2.5.10^{-3}$ mol L^{-1} (straight line) and $0.63.10^{-3}$ mol L^{-1} (dotted lines). NPs size distributions are given as a function of their volume (%).

3.4 Raman spectroscopy

The solid-state Raman spectrum of Pd^0 NPs obtained by reduction of **3** is displayed in figure 6. The solid sample was prepared by precipitation and filtration of POMs-decorated NPs obtained by reduction of a highly concentrated solution of compound **3** (initial concentration of **3** = 5.10^{-3} mol L^{-1}). The spectrum mainly displayed characteristic $\nu_{W=Ot}$ and ν_{W-Ob} bands of heteropolytungstates in the range 750-1000 cm^{-1}. In our case, a large band was observed at 980 cm^{-1}, in addition of some other less intense bands (respectively at 903, 868 and 780 cm^{-1}). The comparison of Pd^0 NPs with the solid-state spectrum of $K_7[PW_{11}O_{39}]\cdot24H_2O$ [25] shows similar spectra. The main difference is due to the degeneracy observed for the band at 980 cm^{-1} in the spectrum of $K_7[PW_{11}O_{39}]\cdot24H_2O$, with two distinct bands at 980 and 965 cm^{-1} (assigned to $\nu_s(W=O_t)$ and $\nu_{as}(W=O_t)$ bands respectively). However, the band patterns

associated to the POMs in both systems are sufficiently close to assert the presence of $[PW_{11}O_{39}]^{7-}$ around the nanoparticles, even after their precipitation.
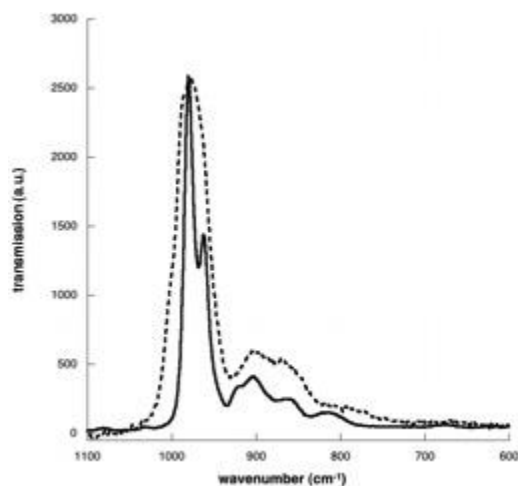

Fig. 6 Raman spectra of $K_7[PW_{11}O_{39}]\cdot 24H_2O$ (straight line) and of Pd^0 NPs obtained by hydrogenation of **3** (dotted line).

3.5 Cryogenic sample preparation and transmission electronic microscopy (Cryo-TEM)

As mentioned by Wang and Weinstock, recent studies on POMs-stabilized metallic NPs focused on the characterization of the composition and nature of the stabilizing shell formed by the POMs.[12] For instance, the direct observation of this shell by classical (HR)-TEM images is hardly achieved, in particular because of the low contrast of non-crystallized materials. Indeed, in the case of dried samples of POMs-stabilized NPs, the NPs generally appeared embedded in a lowly contrasted coating (see fig 2). This situation is amplified by the fact that a large excess of POMs is used in the preparation of the samples. Direct evidences of the presence of POMs in the protecting shell of the NPs were recently obtained by using alternative samples preparations.[18c] Cryogenic techniques were thus used successfully and the cryo-TEM images obtained clearly show the presence of smaller objects on the periphery of the NPs in the case of Ag or Au POMs-stabilized NPs. Before that, we performed cryo-TEM on an aqueous 5.10^{-3} mol L^{-1} solution of $K_7[PW_{11}O_{39}]\cdot 24H_2O$ (fig 7, right). At this concentration we observe the presence of well-isolated dark dots, distributed on the carbon membrane. The diameters of these dots can be estimated to approximately 1.0 nm, compatible with the expected size of single POMs. Figure 7 (left) displays the cryo-TEM micrograph of Pd^0 NPs with **3**. Their shape and size are identical to those observed by (HR-)TEM. Unfortunately, at the concentration of NPs used, we were not able to observe directly the presence of smaller objects that could be attributed to POMs around the NPs, despite the good quality of the micrographs. The presence of POMs can however be detected by EDX spectroscopy on a single nanoparticle as mentioned above.
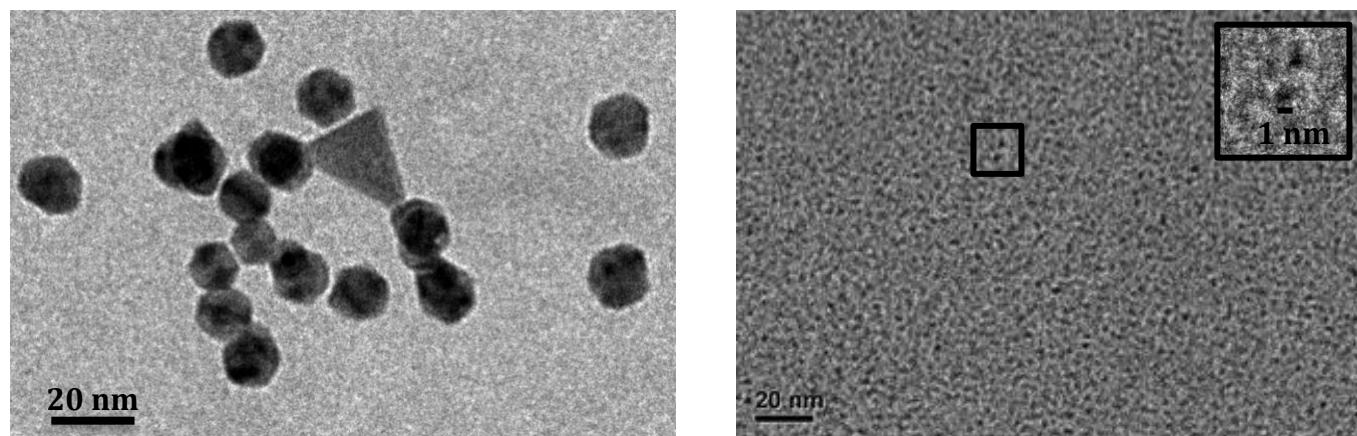

Fig 7: Cryo-TEM micrographs (left) of Nps obtained by hydrogenation of **3** and (right) of a solution of $K_7[PW_{11}O_{39}]\cdot 24H_2O$.

3.6 XPS Characterization.

XPS spectrum has been recorded on a solid sample of Pd^0 NPs stabilized by $[PW_{11}O_{39}]^{7-}$ anions. This sample has been prepared by precipitation and filtration of POMs-decorated NPs obtained by reduction of a highly concentrated solution of compound **3** (initial concentration of **3** = 5.10^{-3} mol L^{-1}, see Raman study, paragraph 3.4). The high resolution Pd3d and W4f spectra are displayed on figure 8. The W 4f peak is composed of a well resolved spin-orbit doublet (35.6 and 37.7 eV for W $4f_{7/2}$ and W $4f_{5/2}$ respectively), typical of W^{VI} atoms in agreement with literature data on Keggin-type POMs.[26] The presence of a single oxidation state on the XPS spectrum clearly indicates the absence of reduction of the POMs sub-units during the NPs genesis and, consequently, the selective reduction of Pd^{II} by H_2. The Pd 3d peak is also composed of a spin-orbit doublet (at 335.2 for $3d_{5/2}$ and 340.5 eV for $3d_{3/2}$) typical of Pd^0 atoms.[27] Both components displayed additional contributions at 336.3 and 341.9 eV (see deconvolution on fig. 8, left) that we have attributed to a surface oxidation of Pd^0 into Pd^{II}.

In addition, K 2p peak was observed and has clearly spaced spin-orbit components (K $2p_{3/2}$ at 292.9 eV and K $2p_{1/2}$ at 295.8 eV (see ESI, fig. S4), confirming the presence of K^+ ions in the materials.
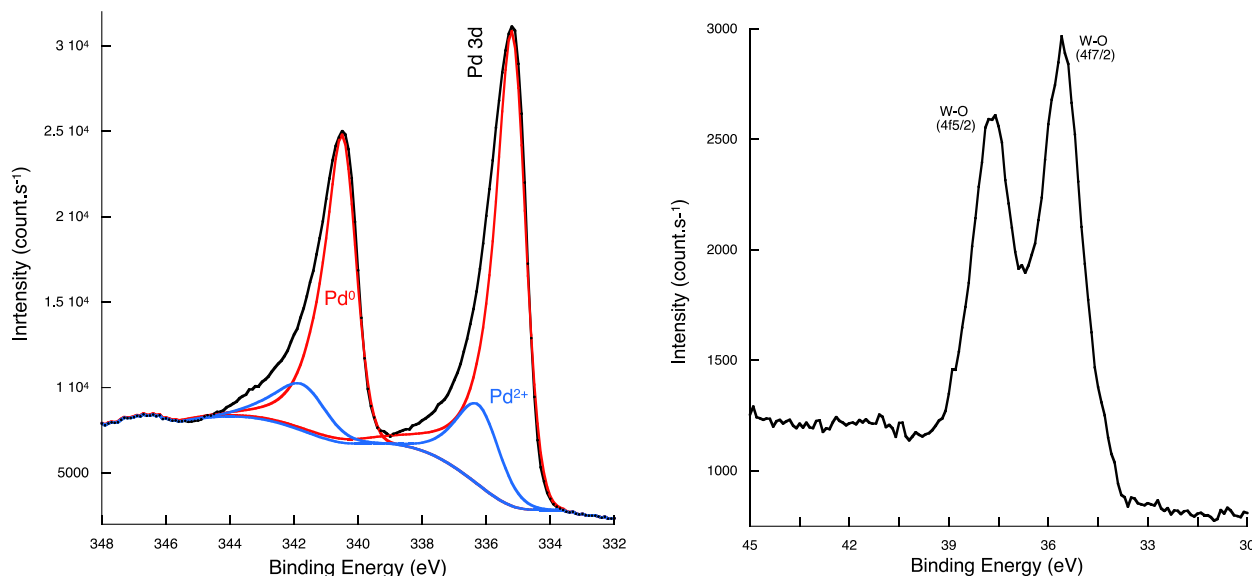

Fig. 8: High resolution Pd3d (left) and W4f (right) spectra of a solid sample of Pd^0 NPs stabilized by $[PW_{11}O_{39}]^{7-}$ anions prepared by precipitation and filtration of NPs obtained by reduction of a highly concentrated solution of compound **3** (initial concentration of **3** = 5.10^{-3} mol L^{-1}).

4. Conclusions

In this study, we have shown that the H_2 reduction of Pd^{II}-POMs derivatives in mild conditions is a simple and efficient reaction that produces reproducible suspensions of lacunary POMs-stabilized Pd^0 NPs in water. This work demonstrates the efficient controlled-synthesis of Pd^0 NPs (as confirmed by XPS) starting from water-soluble non-organometallic Pd^{II}-derivatives, a strategy barely applied until now. In a general way, the ability of the POMs in stabilizing these suspensions was found to be linked to their own integrity in solution. If we compared all tested compounds, the stability of the obtained suspensions can indeed be paralleled to the known stability of the complexing POMs in water. Part of this work is devoted to the thorough characterization of NPs suspensions obtained from **3**. Indeed, we found that the obtained suspensions are stable over several weeks at air with average NPs diameter of approximatively 8 nm. Furthermore the integrity of the $[PW_{11}O_{39}]^{7-}$ anions was confirmed by ^{31}P NMR and Raman spectroscopies. This strategy will be applied to other transition-metal derivatives of POMs in order to obtain suspensions of metallic NPs stabilized with lacunary POMs.

Acknowledgements

Notes and references

[a] Sorbonne Universités, UPMC-Paris 06, UMR 8232, Institut Parisien de Chimie Moléculaire, 4 Place Jussieu, F-75005 Paris, France. E-mail: richard.villanneau@upmc.fr.

[b] CNRS, UMR 8232, Institut Parisien de Chimie Moléculaire, 4 Place Jussieu, F-75005 Paris, France.

[c] Ecole Normale Supérieure de Chimie de Rennes, UMR CNRS 6226, 11 allée de Beaulieu, CS 50837, F-35708 Rennes cedex 7, France.

[d] Université européenne de Bretagne

[e] Sorbonne Universités, UPMC-Paris 06, UMR 7197, Laboratoire de Réactivité de Surface, 4 Place Jussieu, F-75005 Paris, France.

[f] CNRS, UMR 7197, Laboratoire de Réactivité de Surface, 4 Place Jussieu, F-75005 Paris, France.

† A sample of $K_{14}[As_2W_{19}O_{67}(H_2O)]\cdot xH_2O$ (1g, 0.19 mmol) was added to a solution of $Pd(NO_3)_2\cdot xH_2O$ (0.12 g, 0.50 mmol) in 40 mL of 0.5 M acetic acid/sodium acetate buffer (pH = 4.8). The solution was then heated at 80°C for 1h, and filtered on glass wool in order to remove residual solids. Cesium chloride (0.17 g) was then added to the filtrate, which was allowed to stand at room temperature. A brown solid precipitated after a few days and was rinsed with water and ethanol. This solid was used in the hydrogenation reactions without other particular purification. A sample has been recrystallized in hot water to give crystalline materials suitable for an X-ray diffraction study (see ESI for the crystallographic data of compound

$Cs_6K_6[PdAs_2W_{19}O_{67}(H_2O)]\approx 7H_2O$). Elemental analysis, Found: As, 2.37; Cs, 14.30; K, 0.99; Na, 1.23; Pd, 1.98; W, 53.38. Calc. for $As_2Cs_7H_{43.5}K_{1.5}Na_2Pd_1O_{88}W_{19}$ (M = 6258 g mol^{-1}): As, 2.39; Cs, 14.87; K, 0.94; Na, 1.10; Pd, 1.70; W, 55.82%. FT IR, (KBr pellets), cm^{-1}: 945 (s), 885 (vs), 783 (sh), 744 (vs), 690 (sh), 600 (m), 480 (m), 364 (s). Raman (ν (cm^{-1}), solid sample): 960 (vs), 924 (sh), 890 (m), 744 (m).

1   L.D. Rapino, F.F. Nord *J. Am. Chem. Soc.* **1941**, *63*, 2745-2756.

2   (a) G. Somorjai *Chem. Rev.* **1996,** *96*, 1223-1235 (b) *Handbook of Heterogeneous Catalysis*, G. Ertl, H. Knözinger, J. Weitkamp, Wiley-VCH Weinheim, France, **1997**. (c) J. Schulz, A. Roucoux, H. Patin *Chem. Rev.* **2002**, *102*, 3757. (d) D. Astruc, F. Lu, J. R. Aranzaes *Angew. Chem. Int. Ed.* **2005**, *44*, 7852. (e) *Homogeneous hydrogenation: colloids - hydrogenation with noble metal nanoparticles*, A. Roucoux, K. Philippot, in *Handbook of Homogeneous Hydrogenation*, Vol. 1, pp 217-256. Ed. J. G. De Vries, C. J Elsevier. Wiley-VCH, Weinheim, Germany **2007**. (f) S. Schauermann, N. Nilius, S. Shaikhutdinov, H.-J. Freund *Acc. Chem. Res.* **2013**, *46*, 1673-1681. (g) *Metallic nanoparticles in neat water for catalytic applications*, A. Denicourt-Nowicki, A. Roucoux, in *Nanomaterials in Catalysis,* pp 55-95. Ed. P. Serp, K. Philippot Wiley-VCH, Weinheim, Germany **2013**. (h) N. Musselwhite, G. A. Somorjai *Top Catal.* **2013**, *56*, 1277-1283.

3   (a) M. Haruta *CATTECH* **2002**, *6*, 102. (b) *Nanoparticles and Catalysis*, Ed. D. Astruc. Wiley-VCH, Weinheim, Germany **2007**.

4   (a) E. J. García-Suárez, M. Tristany, A. B. García, V. Collière, K. Philippot *Micropor. Mesopor. Mat.* **2012**, *153,* 155-162. (b) P. Maity, C. S. Gopinath, S. Bhaduri, G. K. Lahiri *Green Chem.* **2009**, *11*, 554–561. (c) H. Tsunoyama, H. Sakurai, Y. Negishi, T. Tsukuda *J. Am. Chem. Soc.* **2005**, *127*, 9374-9375. (d) J. Muzart, *Tetrahedron* **2003**, *59*, 5789**.**

5   (a) M. T. Pope Heteropoly and Isopoly Oxometalates, Springer-Verlag, Berlin, 1983. (b) Topical issue on Polyoxometalates: *Chem. Rev.* **1998**, *98*, 1-387 (c) *Polyoxometalates: From Synthesis to Industrial Applications* Eds. M. T. Pope, A. Müller. Kluwer, Dordrecht, The Netherlands, **2001**. (d) A. Proust, B. Matt, R. Villanneau, G. Guillemot, P. Gouzerh, G. Izzet *Chem. Soc. Rev.* **2012**, *41*, 7605-7622.

6   (a) I. V. Kozhevnikov *Catalysis by Polyoxometalates*, Wiley, Chichester, England, **2002**. (b) N. Mizuno, K. Yamaguchi, K. Kanata, *Coord. Chem. Rev.* **2005**, *249*, 1944-1956. (c) C. L. Hill, L.

Delannoy, D. C. Duncan, I. A. Weinstock, R. F . Renneke, R. S. Reiner, R. H. Atalla, J. W. Han, D. A. Hillesheim, R. Cao, T. M. Anderson, N. M.Okun, D. G. Musaev, Y. V. Geletii, *C. R. Chimie* **2007**, *10*, 305-312. (d) Topical issue on POMs in catalysis: Hill C. L. (guest editor), *J. Mol. Cat. A: Chem.* **2007**, *262*, 1-242. (e) R. Neumann *Inorg. Chem.* **2010**, *49*, 3594-3601.

7   (a) O. A. Kholdeeva, G. M. Maksimov, R. I. Maksimovskaya, M. P. Vanina, T. A. Trubitsina, D. Y. Naumov, B. A Kolesov, N. S. Antonova, J. J. Carbo, J. M. Poblet *Inorg. Chem.* **2006**, *45*, 7224-7234. (b) O. A. Kholdeeva *Top. Catal.* **2006**, *40*, 229-243. (c) N. S. Antonova, J. J. Carbo, U. Kortz, O. A. Kholdeeva, J. M. Poblet *J. Am. Chem. Soc.* **2010**, *132*, 7488-7497.

8   (a) Y. V. Geletii, B. Botar, P. Kögerler, D. A. Hillesheim, D. G. Musaev, C. L. Hill *Angew. Chem. Int. Ed.* **2008**, *47*, 3896 –3899. (b) Q. Yin, J. Miles Tan, C. Besson, Y. V. Geletii, D. G. Musaev, A. E. Kuznetsov, Z. Luo, K. I. Hardcastle, C. L. Hill *Science* **2010**, *328*, 342-345.

9   (a) A. Sartorel, M. Carraro, G. Scorrano, R. De Zorzi, S. Geremia, N. D. McDaniel, S. Bernhard, M. Bonchio *J. Am. Chem. Soc.* **2008**, *130*, 5006-5007. (b) F. M. Toma, A. Sartorel, M. Iurlo, M. Carraro, P. Parisse, C. Maccato, S. Rapino, B. R. Gonzalez, H. Amenitsch, T. Da Ros, L. Casalis, A. Goldoni, M. Marcaccio, G. Scorrano, G. Scoles, F. Paolucci, M. Prato, M. Bonchio *Nature Chem.* **2010**, *2*, 826-831.

10 (a) R. Neumann, M. Dahan *Nature* **1997**, *388*, 353-355. (b) M. Bonchio, M. Carraro, A. Sartorel, G. Scorrano, U. Kortz *J. Mol. Cat. A: Chemical* **2006**, *251*, 93-99. (c) R. Neumann, A. Khenkin *Chem. Commun.* **2006**, 2529-2538.

11 S. G. Mitchell, J. M. de la Fuente *J. Mat. Chem.* **2012**, *22*, 18091-18100.

12 (a) Y. Wang, I. A. Weinstock *Chem. Soc. Rev.* **2012**, *41*, 7479-7496. (b) *Polyoxometalate-Protected Sanoparticles: Structure and Catalysis*, Y. Wang, I. A. Weinstock, in *Polyoxometalate Chemistry: Some Recent Trends*. Ed. F. Secheresse, World Scientific Publishing, London, UK, **2013**.

13 (a) Y. Lin, R. G. Finke *J. Am. Chem. Soc.*, **1994**, *116*, 8335-8353. (b) *Transition Metal Nanoclusters,* R. G. Finke, In *Metal Nanoparticles: Synthesis, Characterization, and Applications,* pp 17-237 Eds. D. L. Feldheim, C. A Jr Foss, Marcel Dekker, Inc., New York, Basel, **2002**. (c) H. Weiner, R. G. Finke *J. Am. Chem. Soc.* **1999**, *121*, 9831-842. (d) J. A. Widegren, J. D. Aiken, S. Ozkar R. G. Finke *Chem. Mater.* **2001**, *13*, 312-324. (e) L. S. Ott, R. G. Finke *J. Nanosci. Nanotechnol.* **2008**, *8*,1551-1556. (f) C. R. Graham, L. S. Ott, R. G. Finke *Langmuir* **2009**, *25*,1327-1336.

14 S. Boujday, J. Blanchard, R. Villanneau, J.-M. Krafft, C. Geantet, C. Louis, M. Breysse, A. Proust, *ChemPhysChem* **2007**, *8*, 2636-2642.

15 (a) C. R. Mayer, S. Neveu, V. Cabuil, *Angew. Chem. Int Ed. Engl.* **2002**, *41*, 501-503 (b) N. T. Flynn, A. A. Gewirth *Phys. Chem. Chem. Phys.* **2004**, *6*, 1310-1315. (c) M. De Bruyn, R. Neumann *Adv. Synth. Catal.* **2007**, *349*, 1624-1628. (d) M. A. Alotaibi, E. F. Kozhevnikova, I. V. Kozhevnikov, *Applied catalysis A: General* **2012**, *447-448*, 32-40.

16 (a) B. Keita, T. Liu, L. Nadjo *J. Mater. Chem.* **2009**, *19*, 19-33. (b) G. Maayan, R. Neumann *Chem. Commun.* **2005**, 4595-4597. (c) B. Keita, G. Zhang, A. Dolbecq, P. Mialane, F. Sécheresse, F. Miserque,

L. Nadjo *J. Phys. Chem. C* **2007**, *111*, 8145-8148. (d) J. Zhang, B. Keita, L. Nadjo, I. M. Mbomekalle, T. Liu *Langmuir* **2008**, *24*, 5277-5283.

[17] (a) A. Troupis, A. Hiskia, E. Papaconstantinou *Angew. Chem. Int Ed. Engl.* **2002**, *41*, 1911-1914. (b) S. Mandal, D. Rautaray, M. Sastry, *J. Mater. Chem.* **2003**, *13*, 3002-3005 (c) S. Mandal, A. B. Mandale, M. Sastry, *J. Mater. Chem.* **2004**, *14*, 2868-2871 (d) A. Troupis, A. Hiskia, E. Papaconstantinou *Appli. Catal. B: Environ.* **2004**, *52*, 41-48. (e) C. Costa-Coquelard, D. Schaming, I. Lampre, L. Ruhlmann *Appl. Catal. B: Environmental* **2008**, *84*, 835-842. (f) K. Mori, K. Furubayashi, S. Okada, H. Yamashita *RSC Adv.* **2012**, *2*, 1047-1054. (g) D. Sardar, B. Naskar, A. Sanyal, S. P. Moulik, T. Bala *RSC Adv.* **2014**, *4*, 3521-3528.

[18] (a) A. Z. Ernst, L. Sun, K. Wiaderek, A. Kolary, S. Zoladek, P. J. Kulesza, J. A. Cox *Electroanalysis* **2007**, *19*, 2103-2109. (b) Y. Wang, A. Neyman, E. Arkhangelsky, V. Gitis, L. Meshi and I. A. Weinstock *J. Am. Chem. Soc.* **2009**, *131*, 17412-17422. (c) Y. Wang, I. A. Weinstock *Dalton Trans.* **2010**, *39*, 6143-6152. (d) K. M. Seemann, A. Bauer, J. Kindervater, M. Meyer, C. Besson, M. Luysberg, P. Durkin, W. Pyckhout-Hintzen, N. Budisa, R. Georgii, C. M. Schneider, P. Kögerler *Nanoscale* **2013**, *5*, 2511-2519. (e) Y. Wang, O. Zeiri, V. Gitis, A. Neyman, I. A. Weinstock *Inorg. Chim. Acta* **2010**, *363*, 4416-4420.

[19] V. Kogan, Z. Aizenshtat, R. Popovitz-Biro, R. Neumann, *Org. Lett.* **2002**, *20*, 3529-3532.

[20] R. Villanneau, S. Renaudineau, P. Herson, K. Boubekeur, R. Thouvenot, A. Proust *Eur. J. Inorg. Chem.* **2009**, 479-488.

[21] N. V. Izarova, A. Banerjee, U. Kortz *Inorg. Chem.* **2011,** *50*, 10379-10386.

[22] L.-H. Bi, U. Kortz, B. Keita, L. Nadjo, L. Daniels *Eur. J. Inorg. Chem.* **2005**, 3034-3041.

[23] N. I. Kuznetsova, L. G. Detusheva, L. I. Kuznetsova, M. A. Fedotov, V. A. Likholobov *J. Mol. Cat. A: Chem.* **1996**, *114*, 131-139.

[24] (a) C. M. Tourné, G. F. Tourné *J. Chem. Soc., Dalton Trans.* **1988**, 2411-2420. (b) *General principles of the synthesis of polyoxometalates in aqueous solution*, G. Hervé, A. Tézé, R. Contant, in *Polyoxometalate Molecular Science.* Ed. J. J. Borras-Almenar, E. Coronado, A. Müller, M. T. Pope, NATO Science Series, Vol. 98, Kluwer Academic Publishers, Dordrecht, The Netherlands, **2003**.

[25] C. Rocchiccioli-Deltcheff, R. Thouvenot *J. Chem. Res. (M)* **1977**, 549-571.

[26] D. Mercier, S. Boujday, C. Annabi, R. Villanneau, C.-M. Pradier, A. Proust *J. Phys. Chem. C* **2012**, *116*, 13217-13224.

[27] (a) C. D. Wagner, W. M. Riggs, L. E. Davis and J. F. Moulder, in Handbook of X-ray Photoelectron Spectroscopy, ed. G. E. Muilenberg, Perkin–Elmer Corporation, Eden Prairie, MN, USA, **1978**. (b) L. M. Rossi, F. P. Silva, L. L. R. Vono, P. K. Kiyohara, E. L. Duarte, R. Itri, R. Landers, G. Machado *Green Chem.* **2007**, *9*, 379-385.